RAPID COMMUNICATIONS

PHYSICAL REVIEW C VOLUME 31, NUMBER 5 MAY 1985

Sub-barrier fusion of ^{16}O with $^{16,18}O$

J. Thomas, Y. T. Chen, S. Hinds, K. Langanke, D. Meredith, M. Olson, and C. A. Barnes
Kellogg Radiation Laboratory, California Institute of Technology, Pasadena, California 91125
(Received 21 January 1985)

We have measured the sub-barrier fusion cross sections for the $^{16}O+^{16}O$ and $^{16}O+^{18}O$ systems from $E_{lab}=13.5$–25 MeV. We find no significant enhancement of the $^{16}O+^{18}O$ cross section compared with the $^{16}O+^{16}O$ cross section; this is quite different from the sub-barrier fusion of the calcium isotopes which exhibit a strong isotope dependence.

Sub-barrier heavy ion fusion cross sections are frequently found to be larger than would be expected from simple one-dimensional barrier penetration models that describe elastic scattering. In addition, a strong isotope dependence has been observed in the fusion data of various systems, Ca+Ca and Ni+Ni are prominent examples.[1,2] The explanations proposed for this behavior include collective degrees of freedom, transfer of valence nucleons, and couplings to inelastic channels,[3–5] and the calculations seem to agree qualitatively with the data.[2,6] The oxygen isotopes are particularly interesting with respect to these effects because ^{16}O is a spherical, doubly closed-shell nucleus and one would expect little excitation of shape degrees of freedom at sub-barrier energies, but neutron transfer and inelastic excitation degrees of freedom could still be important for the other oxygen isotopes. The fusion of the oxygen isotopes could therefore provide an ideal test case for the various theoretical approaches aimed at understanding the effects of sub-barrier fusion.

The experiments were carried out with $^{16,18}O^{4+}$ beams from the Caltech EN tandem Van de Graaff accelerator. Data were collected in 0.5 MeV steps in bombarding energy from 13.5 to 25 MeV, and beam currents ranged from 4 μA at the lowest energies to 50 nA at the highest. The large beam currents at low bombarding energy posed a serious problem for the targets due to beam heating and sputtering. Sufficiently rugged targets were made by anodizing[7] thin tantalum sheets to produce a 100 $\mu g/cm^2$ layer of Ta_2O_5. The oxide layer was protected by a 200 $\mu g/cm^2$ layer of gold over each target, and this was sufficient to contain most of the sputtered material. The thickness of each target was estimated from the integrated current required to anodize the tantalum and, in addition, the target thickness was checked by Rutherford backscattering of oxygen ions at low energy. The targets were mounted on a high vacuum beam line with a special water-cooled Conflat flange. Target pressures were maintained in the 10^{-8} Torr range in order to avoid carbon buildup and no observable yield from carbon-oxygen fusion was observed during the course of these experiments. The targets and the detector were surrounded by 10 cm of lead in all directions. The gamma rays resulting from the de-excitation of the evaporation residues were detected with a 100 cm^3 Ge(Li) detector at zero degrees, 0.5 cm behind the target, and the detector efficiency was calibrated with a mixed Eu-Sm source obtained from the National Bureau of Standards. The experimental methods will be described in more detail in a later publication.

The observed γ-ray spectra were composed of lines from the de-excitation of the evaporation residues, Coulomb excitation of the Au and Ta, and room background. The Coulomb excitation lines were easily identified because they were not Doppler shifted, whereas the evaporation residue (ER) lines were Doppler shifted and broadened by as much as 4%. The broadening of the ER lines caused occasional ambiguities in the identification of the gamma rays but, for the $^{16}O+^{16}O$ study, we were able to find at least one unique gamma ray for each of the seven ER resulting from the emission of α, p, n, 2p, 2α, αp, and pn. For the $^{16}O+^{18}O$ study, the α, p, ^{3}He, d or pn, t, 2α, 2n, 2p, αn, and αp channels were uniquely identified. We were unable to identify the ^{3}Heα, nt, αd, and αt channels, but these reactions have large negative Q values and a Hauser-Feshbach calculation indicates that these ER contribute less than 0.1% to the total $^{16}O+^{18}O$ fusion cross section.

The observed γ-ray yields were corrected for summing and branching of the γ decays in the ER, and for the yield directly to the ground states of the ER. The corrections were calculated with a statistical model code, HAUSER*5, [8] to estimate the relative cross sections to the levels below particle threshold and the levels were then depopulated according to the known γ decay branching ratios.[9] The calculated relative yield for each γ ray, β, was then used to correct the observed yield: $\sigma = Y(E_\gamma)/\epsilon(E_\gamma)\beta$, where $Y(E_\gamma)$ is the observed γ yield per incident ion of energy E_γ and $\epsilon(E_\gamma)$ is the detector photopeak efficiency. Finally, the cross sections were corrected for the energy loss of the beam in the targets.

The cross sections for $^{16}O+^{16}O$, $^{16}O+^{18}O$, and the inelastic excitation of ^{18}O are shown in Fig. 1. As has already been observed in the sub-barrier fusion of heavy nuclei, the $^{16}O+^{16}O$ and $^{16}O+^{18}O$ cross sections are found to be enhanced compared with the predictions of barrier penetrabilities as derived from elastic scattering potentials.[10] The present $^{16}O+^{16}O$ cross sections agree well with previous data sets;[11] however, they are about a factor of 2 smaller than those of Hulke *et al.*[12] at the lower energies. In particular we do not find gross oscillations in the $^{16}O+^{16}O$ cross sections as might have been expected from above-barrier elastic scattering and transfer reactions[13] and there is no evidence for unusual structure near $E_{c.m.}=7.5$ MeV as was suggested by Reinhard *et al.*[14] when they compared their calculation with the data of Hulke *et al.*[12]

Our $^{16}O+^{16}O$ data agree well with the cross sections found in an adiabatic time dependent Hartree-Fock calculation (ATDHF)[14] which is presented as the solid curve in Fig. 1. It is interesting to notice that, in the ATDHF calcu-

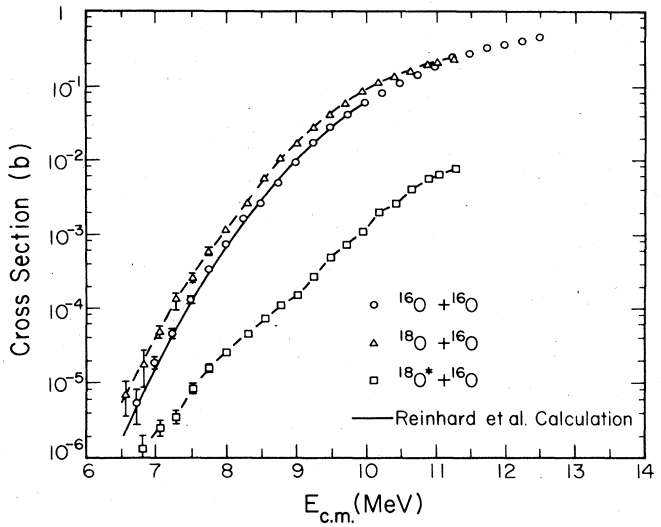

FIG. 1. The cross section for the fusion of ^{16}O with $^{16,18}O$ and the inelastic scattering of $^{18}O^*$.

lation, the enhanced cross section at sub-barrier energies is caused by a radially dependent mass which is greatest for separations just inside the barrier; this corresponds to a potential with a rather thin barrier in the standard potential model using a constant mass parameter. The agreement between theory and experiment is good enough that the calculation can be used to extrapolate the $^{16}O+^{16}O$ fusion cross section down into the astrophysically interesting region at 4 MeV where the S factor is found to be 1.1×10^{26} MeV b. With the S factor given by the present data and the Reinhard *et al.* calculation, the astrophysical (Maxwell-Boltzmann averaged) reaction rate is changed by only 10% from that given by Fowler, Caughlan, and Zimmerman,[15] and thus no major correction is needed for astrophysical purposes.

An interesting feature of the present data is that the $^{16}O+^{18}O$ cross section is only slightly larger than the $^{16}O+^{16}O$ cross section at energies below the barrier. At energies above the barrier, the $^{16}O+^{18}O$ cross section approaches the $^{16}O+^{16}O$ cross section and may even be lower at higher energies. The $^{16}O+^{18}O$ fusion cross section might be expected to be lower if the inelastic cross section or the neutron-transfer cross section increased dramatically at energies above the Coulomb barrier. Unitarity would then require that the fusion cross section decrease. However, this does not seem likely in view of the small inelastic cross section shown in Fig. 1, and because γ-rays from ^{17}O were not detected during the $^{16}O+^{18}O$ experiments indicating that the neutron-transfer cross section was negligible.

The simplest framework within which sub-barrier fusion may be discussed is in terms of a one-dimensional optical potential. Balantekin *et al.*[16] have developed a formalism to invert fusion data to yield the thickness of the potential barrier. Their method is particularly well suited for examining systematic effects in the fusion data because it removes the trivial scaling of the barrier height and radius, and does not introduce assumptions about the shape of the potential. Figure 2 shows the thickness functions for $^{16}O+^{16}O$ and $^{16}O+^{18}O$ plotted as a function of energy below the barrier. Within the experimental error bars, the thickness functions

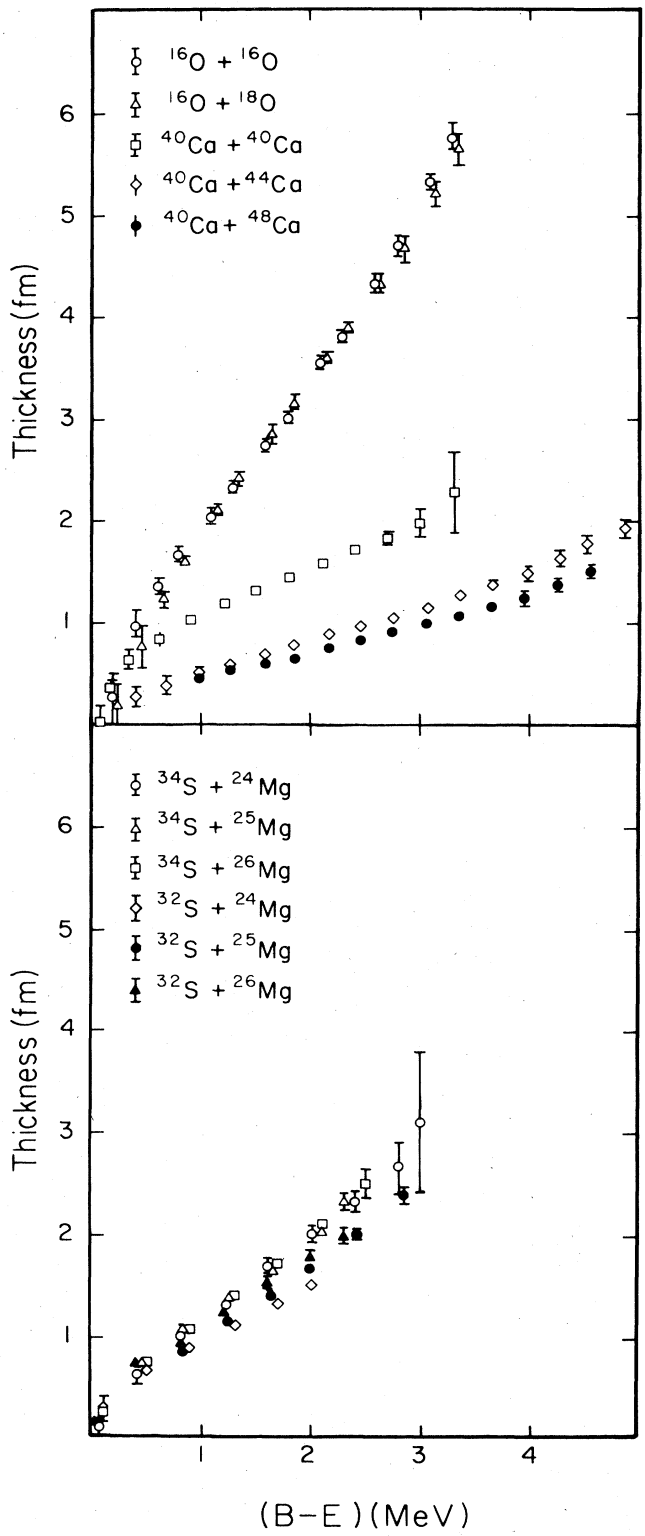

FIG. 2. The thickness functions represent the width of an effective one-dimensional barrier that describes the fusion process. The thickness is plotted as a function of energy below the barrier B. The error bars are shown except when they are smaller than the symbol.

are identical. This suggests that couplings to nuclear degrees of freedom introduced by the two extra neutrons in ^{18}O do not influence the sub-barrier fusion data appreciably.

This result is interesting if we compare it with the $^{24,25,26}Mg + ^{32,34}S$ and $^{40,44,48}Ca + ^{40}Ca$ (Refs. 1 and 17) thickness functions also shown in Fig. 2. There is no observable isotope dependence in the $^{34}S + Mg$ systems and only a weak dependence in the $^{32}S + Mg$ systems. The situation is quite different in the Ca + Ca fusion data. The barrier thicknesses for $^{40}Ca + ^{44}Ca$ and $^{40}Ca + ^{48}Ca$ are similar while the barrier for $^{40}Ca + ^{40}Ca$ is much thicker indicating that adding extra neutrons to the ^{40}Ca core has a significant effect on the sub-barrier fusion data.

If we are willing to make assumptions about the shape of the potential barrier at the outer turning point, then we can use the thickness functions in Fig. 2 to construct the inner side of the barrier and thereby visualize a one-dimensional optical potential which is equivalent to the data in the WKB approximation. Following Inui and Koonin[18] we assumed that the outer barrier is the sum of a Coulomb potential between two point charges and a model nuclear potential. Since the model potential determines the barrier radius, the shape of the inner barrier depends on the choice of the barrier radius. We have calculated the potentials for the oxygen and calcium isotopes as shown in Fig. 3 using the Akyuz-Winther (AW) potential[19] to determine the outer turning point. This is in contrast with the procedure of Inui and Koonin who used the AW potential only for $^{16}O + ^{16}O$; for $^{40,44}Ca + ^{40}Ca$, they chose a smaller barrier radius than is predicted by the AW potential.

As expected from the thickness functions, the $^{16}O + ^{16}O$ and $^{16}O + ^{18}O$ potentials are almost identical except for the scaling due to the different barrier radii. Compared with typical Woods-Saxon potentials derived from elastic scattering, for example, the sub-barrier fusion potentials are more attractive close to the barrier, in qualitative agreement with the results of the ATDHF calculation.[14] The calcium potentials are not so simply related. The addition of the extra neutrons in ^{44}Ca and ^{48}Ca has a dramatic effect on the potential, perhaps reflecting the influence of channel couplings to neutron transfer or inelastic excitations. The $^{40}Ca + ^{44,48}Ca$ potentials show a strong back bend close to the barrier top as has already been observed in potentials derived from $^{64}Ni + ^{64}Ni$ and $^{64}Ni + ^{74}Ge$ sub-barrier fusion data.[16] This back bending may be caused by the attempt to describe complex nuclear degrees of freedom by a simple optical potential. The back bending can be reduced or eliminated by choosing a larger barrier radius than is given by the AW potential, but the larger radius and resulting lower barrier may also be interpreted as resulting from the attempt to describe many degrees of freedom by a one-dimensional potential.

In summary, the sub-barrier fusion of ^{16}O with $^{16,18}O$ can be described by a simple one-dimensional potential barrier which, however, is thinner than would be expected from elastic scattering, and the small isotope shift seen in the data can be accounted for by scaling the potential for the different barrier heights and radii of ^{16}O and ^{18}O. This result is quite different from the behavior of the sub-barrier fusion of the calcium isotopes which exhibit a strong isotope

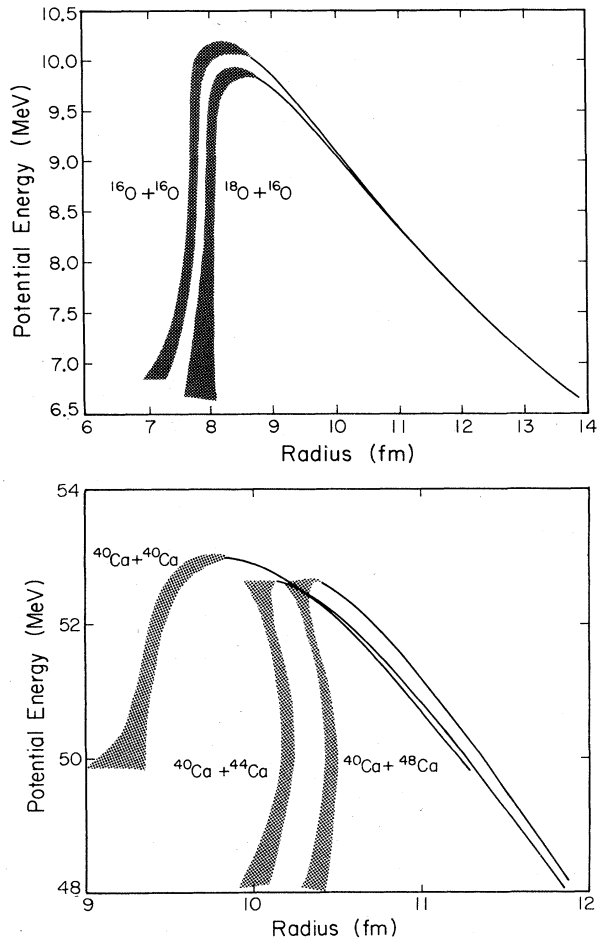

FIG. 3. The effective one-dimensional barriers for $^{16}O + ^{16,18}O$ and $^{40}Ca + ^{40,44,48}Ca$ fusion using the thickness functions in Fig. 2 and the AW potential to determine the shape of the outer barrier. The shaded regions represent the uncertainty in the barrier thickness due to the experimental errors in the cross section.

dependence with the $^{44,48}Ca + ^{40}Ca$ data being much larger than the $^{40}Ca + ^{40}Ca$ cross section. To understand the differences in the sub-barrier fusion for the oxygen and calcium isotopes, it is important to study the sub-barrier fusion of other oxygen isotopes, for example, $^{17}O + ^{16}O$ and $^{18}O + ^{18}O$. We expect that all of these data taken together will help to constrain theories that predict an enhancement of the sub-barrier fusion cross section due to couplings to neutron transfer and inelastic scattering channels. Measurements of the sub-barrier fusion of these other oxygen isotopes are currently under way.

One of us (J.T.) is grateful for support by a Millikan Fellowship from the California Institute of Technology. We would like to thank Baha Balantekin and Steven Koonin for useful discussions. This work was supported in part by the National Science Foundation, Grant No. PHY 82-15500.

[1]H. Al-Juwair *et al.*, Phys. Rev. C **30**, 1223 (1984).
[2]M. Beckerman *et al.*, Phys. Rev. C **28**, 1963 (1983).
[3]H. Esbenson, Nucl. Phys. **A352**, 147 (1981).
[4]H. J. Krappe *et al.*, Z. Phys. A **314**, 23 (1983).
[5]S. Landowne, in *Proceedings of the International Conference on Fusion Reactions Below the Coulomb Barrier, Cambridge, 1984,* edited by S. G. Steadman (Springer-Verlag, Berlin, 1985).
[6]S. Landowne and S. C. Pieper, Phys. Rev. C **29**, 1352 (1984).
[7]D. Phillips and P. S. Pringle, Nucl. Instrum. Methods **135**, 389 (1976).
[8]F. M. Mann, Hanford Engineering and Development Laboratory Report No. HEDL-TME 78-83, 1978 (unpublished).
[9]P. M. Endt and C. Van Der Leun, Nucl. Phys. **A214**, 1 (1973).
[10]P. R. Christensen, R. E. Switkowski, and R. A. Dayras, Nucl. Phys. **A280**, 189 (1977); W. von Oertzen and H. G. Bohlen, Phys. Rep. **19C**, 1 (1975).
[11]C. S. Wu and C. A. Barnes, Nucl. Phys. **A422**, 373 (1984), and references therein.
[12]G. Hulke, C. Rolfs, and H. P. Trautvetter, Z. Phys. A **297**, 161 (1980).
[13]G. Gaul, W. Bickel, W. Lahmer, and R. Santo, in *Resonances in Heavy Ion Reactions,* edited by K. A. Eberhard, Lecture Notes in Physics, Vol. 156 (Springer, Berlin, 1982), p. 72; G. Gaul (private communication).
[14]P. G. Reinhard *et al.*, Phys. Rev. C **30**, 878 (1984); also, R. Gissler *et al.* (unpublished).
[15]W. A. Fowler, C. R. Caughlan, and B. A. Zimmerman, Annu. Rev. Astron. Astrophys. **13**, 69 (1975); W. A. Fowler (private communication).
[16]B. Balantekin, S. Koonin, and J. Negele, Phys. Rev. C **28**, 1565 (1983).
[17]G. M. Berkowitz *et al.*, Phys. Rev. C **28**, 667 (1983).
[18]M. Inui and S. E. Koonin, Phys. Rev. C **30**, 175 (1984).
[19]O. Akjuz and A. Winther, in *Proceedings of the Enrico Fermi International School of Physics, 1979,* edited by R. A. Broglia, C. H. Dasso, and R. A. Ricci (North-Holland, Amsterdam, 1980), p. 492.